IAHR AIRH

Journal of Hydraulic Research Vol. 45, No. 5 (2007), pp. 653–660

Laboratory tests on self-excitation of concentration fluctuations in slurry pipelines

Essais en laboratoire sur l'auto-excitation des fluctuations de concentration dans des tuyaux de refoulement

A.M. TALMON, Senior Researcher/Advisor, *Delft Hydraulics, P.O. Box 177, 2600 MH Delft, The Netherlands and Delft University of Technology, Faculty of Mechanical, Maritime and Materials Engineering, Mekelweg 2, 2628 CD Delft, The Netherlands. E-mails: arno.talmon@wldelft.nl or a.m.talmon@tudelft.nl (author for correspondence)*

L. AANEN, Researcher/Advisor, *Delft University of Technology, Faculty of Architecture, Berlageweg 1, 2628 CR Delft, The Netherlands and Peutz BV, P.O. Box 66, 6585 ZH Mook, The Netherlands. E-mails: L.aanen@tudelft.nl or L.aanen@mook.peutz.nl*

R. BAKKER-VOS, Reliability Engineer, *DSM Melamine, P.O. Box 43, 6130 AA Sittard, The Netherlands. E-mail: regje.bakker-vos@dsm.com*

ABSTRACT

High concentration solid–liquid mixtures that are conveyed by pipeline have been found to develop large amplitude concentration fluctuations. A closed-loop laboratory circuit is used to investigate the mechanism of self-excitation. According to linear stability theory these concentration fluctuations originate from an adverse relation between the settling flux and solids concentration. Concentration variations amplify due to solids exchange with a bed layer. The internal structure of the flow is investigated by means of concentration profile measurements. The measurements show that self-excited harmonic perturbations quickly deform into sawtooth shape concentration variations. An explanatory non-linear theory is given.

RÉSUMÉ

Il a été observé que des mélanges solides–liquides de haute concentration transportés dans des tuyaux développaient d'importantes fluctuations de leur concentration. En laboratoire, un circuit fermé est utilisé pour étudier le mécanisme d'auto-excitation. Selon la théorie de stabilité linéaire, ces fluctuations trouveraient leur origines dans la relation inverse entre la concentration en solide du mélange et sa vitesse de sédimentation. Des variations de la concentration se voient amplifiées par l'échange de particules solides avec le lit de fond. La structure interne de l'écoulement est étudiée grace à des mesures de profilés de concentration. Des mesures montrent que les perturbations harmoniques, auto-excitées se transforment rapidement en variations de concentration en forme de dents de scie. Une explication de ce phénomène, basée sur une théorie non-linéaire, est proposée.

Keywords: Slurry, pipeline, sand-water-mixtures, density waves, linear stability.

1 Introduction

Pipeline transport of highly concentrated solid–liquid mixtures is on many occasions more cost-effective than transport by other means. Traditionally slurry pipeline research has been focused on steady-state conditions. In practise however dynamic variations are becoming more and more a problem. These variations might be due to variations in feed or operating conditions, but these might also be due to other mechanisms.

One such mechanism is self-excitation of concentration fluctuations. This phenomenon has been brought to the attention of the international scientific community by Dr Matousek of Delft University. Matousek (1997) reported on an amplification of concentration variations along the length of a long distance dredge pipeline. At the exit of the pipeline the slurry density varied dynamically between 1000 and 1500 kg/m^3. The pipeline was 10 km long with a nominal diameter DN650. Highly concentrated sand–water mixtures were pumped to a highway construction site near The Hague, The Netherlands. This transportation system was operated close to the limit deposit velocity to prevent deposition and to refrain from unstable conditions. The measurements showed that high-frequency concentration variations were damped, while low frequency variations were amplified. The propagation velocity of concentration variations nearly equalled the flow velocity, their wavelength was about 1 km.

To explain self-excitation, a linear perturbation analysis was employed to determine the influence of the various internal processes, Talmon (1999). The analysis involved a two-layer schematisation of the flow: a bed layer and a suspended load layer, (see Fig. 1). As a result the hindered settling of solids at

Revision received December 28, 2001/Open for discussion until April 30, 2008.

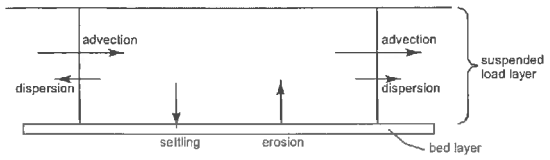

Figure 1 Definition sketch internal processes in pipeline transport.

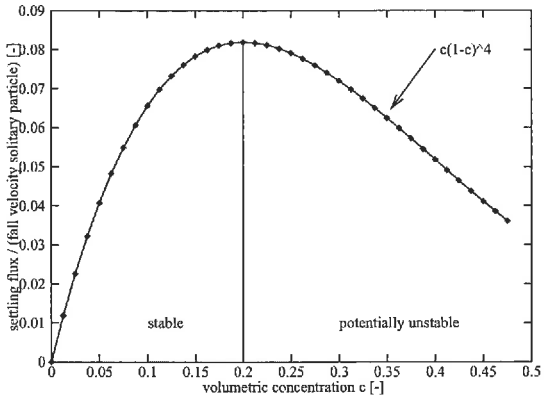

Figure 2 Settling flux as a function of solids concentration.

high concentrations was identified as the cause of the amplification of concentration variations. The reason is an adverse relation between the settling flux and solids concentration, for solids concentrations greater than 20% (Fig. 2). Because of the smoothing action of axial dispersion an amplification is only possible at large wavelengths.

The most important hypothesis in the theory is that hindered settling effects are stronger than the influence of the suspended load concentration on erosion. Measurements in a laboratory circuit, van Rhee and Talmon (2000), confirmed that hindered settling dominates over hindered erosion. The latter process was identified earlier by Winterwerp *et al.* (1990).

Matousek (2001) further analysed the pipeline data mentioned above, and used the self-excitation theory as a basis to quantify the development of density waves.

According to the theory the density wave amplification process manifests itself preferably in relatively lengthy pipelines. These might be long distance pipelines as well as short distances in case of minute tubes. Density amplification might also play a role in recirculating solids flow systems such as in fluidisation and other suspension processes. These types of flow occur in dredging, processing industry, mining industry and diverse civil engineering applications. If the possibility of density wave amplification is not considered in the design of solids transport systems, difficulties such as overload and shut-down, might arise.

The goal of the laboratory experiments presented in this paper is to verify the theory by arousing the instability, to find limiting conditions and to investigate its relation with different types of solids transport regimes.

2 Closed-loop slurry instability testing

2.1 *Closed-loop testing*

In long distance pipelines density waves with the strongest amplification rate prevail. This wave-number selection process is impractical to test, because this would demand a very lengthy laboratory circuit. However a shorter closed-loop circuit will also provide the necessary information, provided the length of the circuit is longer than the critical wavelength for density amplification.

2.2 *Capabilities and limitations of the linear theory*

The linear perturbation theory considers the (in)stability of coupled internal processes. The average internal process conditions are input to the theory. The linear theory tells us whether small perturbations of the internal structure will amplify or not. It also gives the growth rate of perturbations in the initial phase of amplification. At present the (in)stability theory predicts that self-amplifying density waves might develop at high concentrations in presence of a stationary or sliding bed layer. This is to be verified.

It was not known whether the instability also occurs in the fully suspended heterogeneous flow regime. The maximum concentration being attained by the amplifying density waves is an other unknown. It is conceivable that at high concentrations non-linear interactions might prohibit further amplification. Such interactions are not addressed by the linear perturbation theory. It is further expected that at concentrations greater than 40% granular processes might take over, and density wave amplification is halted.

3 Laboratory experiments

3.1 *Closed-loop laboratory circuit*

A laboratory circuit with a total length of about 52 m and an internal diameter of 100 mm is used. The circuit is sketched in Fig. 3. The circuit consists of two 25-m horizontal pipes, both at an elevation of about 1 m above the floor and the distance between the pipes is 0.6 m. Characteristic parameters of the sand being used are: $d_{50} = 200\ \mu$m and $d_{85}/d_{50} = 1.9$ (see Fig. 4).

The flow is driven by a centrifugal pump located at one end of the circuit. At the other end the flow is diverted back by means of two closely spaced bends. The pump and pipes are connected by flexible pipes of about 1 m length. The rotation speed of the slurry pump is controlled electronically.

A standpipe is situated near the inlet of the pump. Sand supply and drain openings are located about 10 m downstream of the pump.

The end of the second pipe consists of a 6-m-long observation section. Visual observation of the bed at the bottom of the pipe, and its character (stationary or sliding), is important. Close

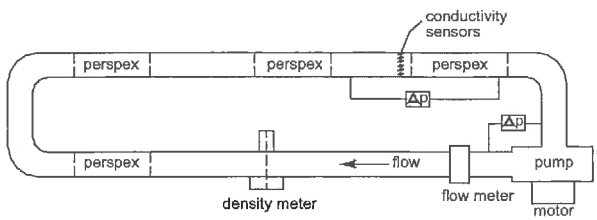

Figure 3 Sketch of laboratory circuit, not to scale.

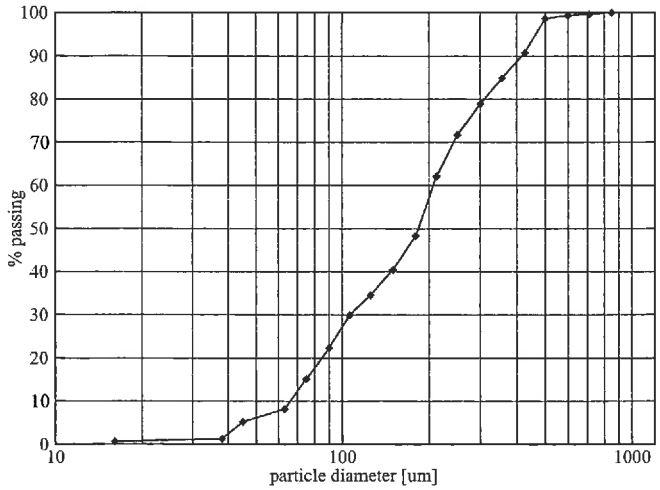

Figure 4 Sieve curve of sand.

the entrance of this perspex section (0.3 m upstream) a set of conductivity probes is installed to measure the concentration distribution over the circumference of the pipe. At the opposite end of the circuit two shorter observation sections are present. Another observation section is located halfway of the second pipe. The purpose of these sections is to monitor downstream variation of transport processes.

The flow rate is measured by an electro-magnetic flow meter. The flow meter is located 2.5 m downstream of the pump. Pressure losses are measured by differential pressure transducers. One transducer measures the hydraulic pressure loss over the main observation section. Pressure tappings are 10 m apart. The total hydrodynamic resistance of the circuit is measured by the second transducer measuring the pressure difference over the pump.

The density of the mixture is determined by a radioactive transducer, located about 18 m downstream of the pump. The average density at half pipe height is measured. Also samples are taken and the sand content was determined. The set of conductivity probes mentioned above consists of 16 pairs of electrodes distributed over the circumference of the pipe. Six of these are located near the bottom of the pipe to detect the presence of a bed layer. The temperature of the sand–water mixture was measured by an electronic thermometer.

3.2 Measuring programme

Four mixture concentrations have been tested. Each mixture concentration was first tested from $U = 0.5$ to 6 m/s, by stepwise increasing the rpm of the pump. Each rpm-setting was tested for about 3 min. The purpose of these measurements was to determine the flow resistance and to identify characteristic transitions of sediment transport regime. In particular the full suspension transition could be distinguished clearly, both visually and by the conductivity probes at the bottom of the pipe.

Next the critical flow velocity for density wave development was determined. In the first tests the density meter showed that the critical conditions for density wave development were close to the full suspension transition. Around these conditions ($\sim$ 2 m/s) more tests were conducted at a velocity interval of about 0.05 m/s. Finally some typical flow velocities were selected to capture the dynamics of density wave amplification in more detail. The duration of the latter experiments was about 10–20 min.

Before each test the circuit was run at a higher flow velocity to homogenise the solids concentration along the length of the circuit. Major density variations are caused at start-up of the pump, but density variations may also result from continuation after an earlier test in which density waves were generated. When, according to the density meter, the perturbation had vanished the rpm of the pump was gradually reduced until the desired test conditions were reached.

4 Results

4.1 Phenomenological description of test results

At the lowest flow velocities a flat stationary bed is observed in all perspex sections. At higher flow velocities the thickness of the bed layer decreases, but after some revolutions of the flow the bed level starts to vary in concert with the density meter and conductivity probes. Density waves develop within a few revolutions of the mixture through the circuit. Major concentration variations occur when the process is allowed to continue. Their amplitude is about half the mean mixture concentration. If next the velocity is increased, up to conditions where there is no bed layer anymore, the concentration fluctuations diminish slowly (10 min are needed to homogenise). In absence of a bed layer the flow and sediment transport are stable.

Starting with high flow velocities, density wave development commences slightly below the critical velocity for transition to a stationary bed, when the bed has a width of about 5 cm. A fixed operating point of pump and circuit is attained, or the flow rate drops until a new operating point is reached where the pump curve and the resistance curve of the circuit intersect sharply again (Table 1).

From visual observation and recorded data the following characteristic flow velocities are found in the experiments:

When, starting again at high velocities, the flow rate is reduced, the first visual occurrence of the "bed layer" coincides with detection at the conductivity probes. Under those conditions the concentration profile is strongly stratified. The concentration of the suspension near the bottom is of the order 40–50 v%. The concentration in the upper part of the pipe is about 5–15 v% depending on mean concentration.

Table 1 Characteristic flow velocities

	Incipient density wave development U_{cr} (m/s)	Transition: stationary bed layer/thin layer of sliding grains U (m/s)	Full suspension U (m/s)
14 v%	1.93	2.04	2.14
18 v%	1.81	2.01	2.21
25 v%	1.6 Q-shift system	2.01	2.27
30 v%	1.25 Q-shift system	1.86	2.25

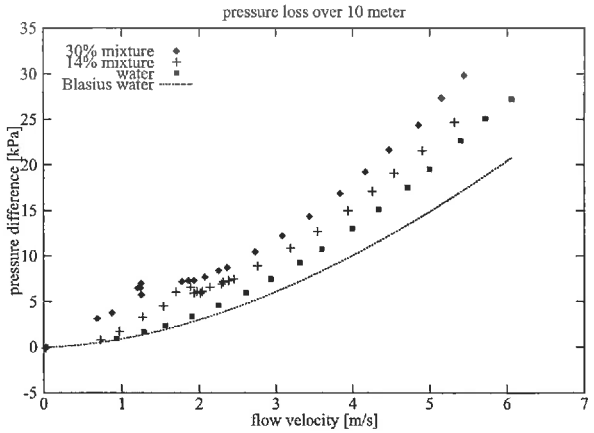

Figure 5 Flow resistance measured over straight pipe section.

En mass sliding bed conditions did not occur in the tests. Only thin sliding patches of grains were observed before full suspension was reached. Their movement is irregular. At the lowest concentrations the transition of a stationary bed to sliding patches of grains and the subsequent full suspension condition occurred at nearly the same flow velocity. At the highest concentrations corresponding flow velocities differed more.

4.2 Flow resistance

An example of the measured pressure drop over the straight pipe section is given in Fig. 5. To compare the results, the theoretical resistance curve for hydrodynamic smooth conditions, according to Blasius, is also included. At standstill all sand is within the bed layer. Starting at small flow velocities the resistance increases with flow velocity. The thickness of the bed layer however decreases because sand is entrained in the flow. In the velocity range $1.3 < U < 1.8$ m/s no stable operating point is possible at 30 v%. Such conditions occur also at 25 v%, although the velocity range is smaller.

4.3 Internal structure of the flow

Time-averaged concentration profiles

Two examples of time-averaged concentration profiles are given in Figs. 6(a) and (b). These were constructed from concentration measurements by the conductivity probes. The flow conditions concern the transition to a stationary bed, higher flow velocities and lower velocities at which density waves are present. The measuring period is about 5 min.

The time series of the conductivity probes showed high-frequency fluctuations when local concentrations are smaller than 40–50 v%. This is attributed to turbulence. The highest concentrations are measured near the bottom. At velocities smaller than the critical velocity a stationary bed layer is observed (concentrations ~ 55–60%). Inspection of the time series reveals that the concentrations measured in the bed are nearly constant. Above the critical flow velocity the shape of the concentration profile varies gently with the flow velocity. When a formidable bed layer has formed, such as under conditions of 25–30 v%, the concentration profile is heavily stratified (Fig. 6b).

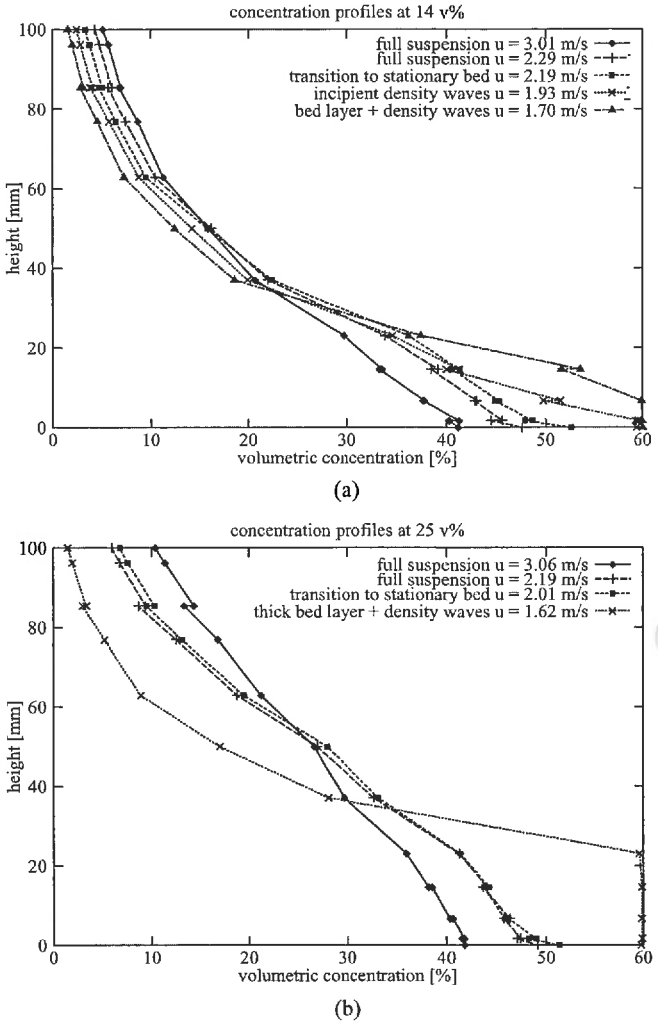

Figure 6 Examples of solids concentration profiles.

Dynamic variations

Two typical time series of concentration measurements are given in Figs. 7(a) and (b). The very first part of the time series concern conditions with the pump not being started yet. Next the solids distribution along the length of the circuit is being homogenised by running the circuit at full speed (~ 50 l/s) for a duration of about 5 min. As a consequence the temperature of the mixture increases. The output of the conductivity probes changes accordingly. Next the rpm of the pump is lowered to the point of incipient instability. At these conditions the development of density fluctuations is very clear. Small amplitude harmonic density variations, having a period equal to the circulation time of the flow, develop into larger amplitude sawtooth-shaped density waves within one to three revolutions of the mixture through the circuit. The amplitude of the concentration variations is largest at half pipe height. Concentration variations at the bottom are smaller. Concentration variations at the crest of the pipe are very small.

At the end of each test, when the pump was shut of, the data registration continued for 1 or 2 min to allow for a recalibration of the conductivity probes afterwards.

The height of the bed layer is observed to vary with passage of density waves. This illustrates that erosion and sedimentation

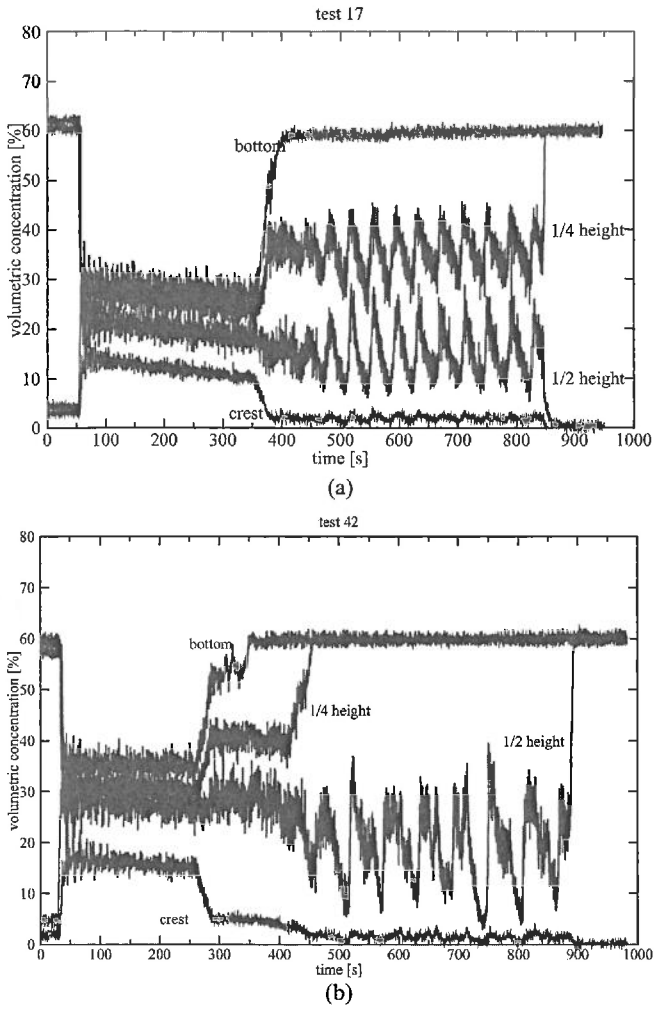

Figure 7 Examples of concentration fluctuations at instability.

processes at the bed surface are involved. The bed level increases relatively fast on the approach of the high concentration at the front of the density wave. During passage of the density wave the bed level decreases again slowly.

Variations of the pressure difference over the main observation section are in phase with passage of the sawtooth waves over the conductivity probes. Pressure variations over the pump are small.

At a mean solids concentration of 14 v% a very regular sawtooth-shaped density wave was found that travelled at a celerity of 1.3 m/s, which is about 70% of the mean flow velocity. At higher mixture concentrations the concentration variations are less regular. The impression is that two shorter sawtooth waves developed in the circuit in combination with subharmonics. Celerities of the former are 75–95% of the mean flow velocity. The celerity of the latter is about half the speed of the mean flow. The amplitude of these subharmonics is significant and are accompanied by major variations of the surface level of the bed layer.

4.4 Flow conditions at incipient instability

Density wave amplification starts when the bed has grown a little. This has been observed at mean solid concentrations of 14 and 18 v%. At higher concentrations the situation is different. The flow rate drops together with the build up of a thicker bed layer. The associated hydrodynamic conditions are listed in Table 2.

The calculated fall velocity of a solitary particle is $w = 25$ mm/s. The Darcy–Weisbach friction factor is calculated from

$$f = 2\frac{D}{L}\frac{\Delta p}{\rho U^2}$$

with D = pipe diameter, L = distance between pressure fittings, Δp = pressure drop over straight pipe section, ρ = mixture density. The wall shear stress is calculated from:

$$\tau_w = \frac{D}{4}\frac{\Delta p}{L}$$

The wall shear velocity is defined by: $u_* = \sqrt{\tau_w}/\rho$.

4.5 Summary of main results of the experiments

The self-excitation phenomenon occurred in the experiments, and means to arouse these and how to control these were tested.

A thin bed layer is sufficient for density wave development to commence.

Table 2 Flow conditions at incipient instability (at stationary operating point of pump and circuit)

	Test 17	Test 28	Test 42	Test 58	Unit	Remark
Mean solids concentration $\bar{c}$	14	18	25	30	v%	
Mean density mixture ρ	1225	1300	1410	1500	kg/m^3	
Mean flow velocity U	1.93	1.81	1.62	1.25	m/s	
dp/dx (straight pipe)	0.61	0.67	0.86	0.70	kPa/m	Main observation section
Δp (over pump)	31.0	32.4	34.9	35.5	kPa	
h_{bed}	10	25	30	40	mm	Approximately
Wave amplitude Δc	15	15	23	32	v%	Approximately at $z = 50$ mm
Wave speed	1.3	1.5	1.2	1.2	m/s	Approximately
Friction coefficient f	0.0257	0.0315	0.0465	0.0597	—	Darcy–Weisbach
Wall shear stress τ_w	15.3	16.8	21.5	17.5	Pa	Average of circumference
Wall shear velocity u^*	0.111	0.114	0.123	0.108	m/s	Average of circumference
Temperature mixture	28.6	31.7	28.2	27.6	°C	

At low concentrations the limiting velocities for a stationary deposit and "full suspension" nearly coincide. At the highest concentrations corresponding flow velocities differ more, because of a widening of the intermediate regime with sliding patches of grains.

5 Evaluation

5.1 Concentration profile

At the investigated conditions the concentrations above the bed are of the order 30–40 v%, consequently the adverse relation between solids concentration and settling flux is involved (see Fig. 2). These measurements show that bottom concentrations are large enough to initiate density wave development.

The suspended load concentration close to the bed layer, or at the bottom of the pipe, varies only marginally with mean concentration. According to the linear theory small variations are already sufficient to initiate density wave development.

5.2 Self-excitation of density waves

The development of initial small harmonic waves was predicted by the slurry instability theory of Talmon (1999). It is caused by the adverse relation between settling flux and solids concentration in combination with the presence of a (sliding) bed layer. Matousek's (2001) re-evaluation of the dredge pipeline data showed that density waves are amplified whenever there is a bed layer. Contrary to our data it also occurred for sliding bed layer conditions.

Furthermore, the transition into sawtooth-shaped density waves is probably caused by variable slip of solids transport with respect to the flow. The underlying mechanism is then that at high concentrations the concentration profile is more uniform, and consequently the celerity of these high concentrations is the greatest. Matousek (1997) identified the variable slip phenomenon in both the dredge pipeline and in his laboratory measurements.

5.3 Other data on density fluctuations

Instrumentation of the bottom of pipelines has been pursued in the past to detect the formation of bed layers. Ercolani *et al.* (1979) employed electric and thermal probes. Under laboratory conditions they observed a regular fluctuating pattern at the limit deposit velocity (visual observation in $D = 53$ mm perspex pipe section). Also Klose (1984) installed probes at the bottom of a laboratory pipeline as an aid to detect the deposit limit. In both investigations the attention was focused on concentration variations due to erratic behaviour of the bed layer.

According to our experiments, fluctuating concentrations are not the key indicator for bed layer development. On the contrary, on first formation of the bed layer, the concentration at the bottom of the pipe increases and attains a high and constant value.

6 Non-linear theory for sawtooth waves

The continuity equation of suspended load transport governs the time and spatial development of suspended load concentrations:

$$\frac{\partial \bar{c}}{\partial t} + U\frac{\partial \alpha \bar{c}}{\partial x} + \frac{BD}{A}\frac{w_s c_b - E}{D} = \varepsilon \frac{\partial^2 \bar{c}}{\partial x^2} \tag{1}$$

with: A = suspended load area, B = width of bed, c_b = near bed concentration, E = erosion rate, w_s = fall velocity solids, α = variable slip coefficient, ε = axial dispersion coefficient. The variables U, c, and ε are related to the suspended load part of the flow.

A typical mathematical expression for axial dispersion in straight pipes is: $\varepsilon = 5u_* D = 5\sqrt{f/8}UD$ (Taylor, 1954). Axial dispersion in bends and pumps is smaller than in straight pipe sections (Murakami *et al.*, 1985).

As will be shown, the sawtooth waves are governed by non-linear advection and the adverse relation between the sedimentation flux and concentration. The variable slip coefficient in the advection term is approximated by a linear function: $\alpha = a + b\bar{c}$. The cross-sectional average concentration is modelled by: $\bar{c} = \bar{c}_0 + \bar{c}'$, in which $\bar{c}_0$ is the time and spatial average, and $\bar{c}'$ is the variation of the cross-sectional average concentration. Substitution in the continuity equation and linearisation of the settling flux gives:

$$\frac{\partial \bar{c}'}{\partial t} + U(a + 2b(\bar{c}_0 + \bar{c}'))\frac{\partial \bar{c}'}{\partial x} + \frac{BD}{A}\frac{w_{s0}}{D}\phi c_b' = \varepsilon \frac{\partial^2 \bar{c}'}{\partial x^2} \tag{2}$$

with: c_b' = variation of near bed concentration, w_{s0} = average fall velocity of solids at bed level: $w_{s0} = w(1 - c_{b0})^\beta$, in which: β = hindered settling exponent, c_{b0} = average concentration at bed level, and

$$\phi = \frac{1 - (1 + \beta)c_{b0}}{1 - c_{b0}} \tag{3}$$

The solution is a sawtooth-shaped wave, for a definition sketch see Fig. 8. The propagation velocity of this wave is: $V = (a + 2b\bar{c}_0)U$. The concentration variation, for $-1/2L < x < 1/2L$, is given by: $\bar{c}' = \frac{\Delta c}{2}\left(1 + \frac{2x}{L}\right)$, with: Δc = maximum concentration difference, and L = length of sawtooth wave. The time-development of Δc is given by:

$$\frac{\partial \Delta c}{\partial t} = -\frac{2bU}{L}(\Delta c)^2 - \frac{BD}{A}\frac{w_{s0}}{D}\frac{c_b'}{\bar{c}'}\phi \Delta c \tag{4}$$

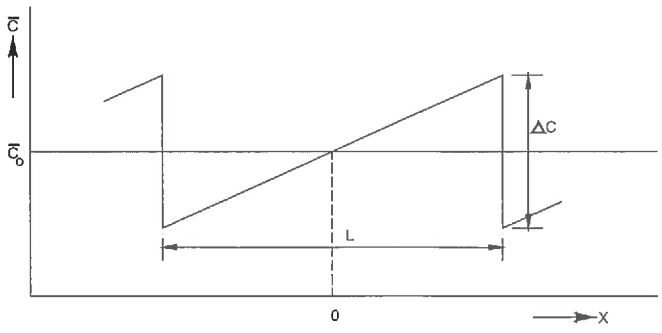

Figure 8 Definition sketch sawtooth shape concentration variation.

After a short time an equilibrium is reached and Δc is given by:

$$\Delta c = \frac{-1}{2b}\frac{L}{D}\frac{BD}{A}\frac{w_{s0}}{U}\frac{c'_b}{\bar{c}'}\phi \tag{5}$$

These mathematical equations are similar to the non-linear Burgers equation of 1940 (see Nieuwstadt and Steketee, 1995).

Typical values for the parameters of non-linear advection and the variation of the near-bed concentration that apply to the experiments are: $a = 0.6$, $b = 0.4$, $\beta = 4$, $c_{b0} = 0.5$ and $c'_b/\bar{c}' = 0.2$. These values are of course a function of the actual state of the suspended load process and have no general validity. Using these values the calculated maximum concentration difference of the sawtooth waves is 20 v% ($\Delta c = 0.2$), the order of magnitude of which is in agreement with the measurements.

It is concluded that non-linear advection, in combination with an adverse relation between settling flux and concentration, governs the maximum amplitude of concentration fluctuations. The presence of a bed layer is a necessity.

7 Conclusions

In the reported experiments the fundamental mechanism of density wave amplification occurring in long distance solids transportation pipelines has been investigated under controlled conditions. Slurry instabilities occurred at each tested solids concentration (test range 14–30 v%).

The self-excitation of density waves commences whenever there is a thin bed layer. According to linear theory, these instabilities are caused by an adverse relation between the settling flux and concentration in combination with the presence of a bed layer. The measured internal structure of the flow, and its dynamic variation, are in accordance with the premises of the linear theory. No density amplification phenomena were observed in the full suspension regime.

Harmonic concentration fluctuations were found to deform quickly into large amplitude sawtooth-shaped concentration fluctations. This process cannot be explained by linear theory. Non-linear theory shows that non-linear advection, in combination with the adverse relation between the settling flux and the concentration, governs the deformation of density waves and determines the maximum amplitude of concentration fluctuations. A bed layer is necessary for the density waves to feed upon.

Acknowledgment

The authors gratefully acknowledge that permission to publish was granted by the polyolefin division of DSM Research B.V. (now Sabic Europe).

Notation

A	=	Cross-sectional area suspended load transport	(m^2)
a	=	Coefficient in variable slip model	(–)
B	=	Width of bed layer	(m)
b	=	Coefficient in variable slip model	(–)
c	=	Volumetric concentration	(–)
c_b	=	Near bed concentration	(–)
$\bar{c}$	=	Mean solids concentration	(–)
$\bar{c}_0$	=	Time and spatial average	(–)
$\bar{c}'$	=	Variation of the cross-sectional averaged concentration	(–)
c'_b	=	Variation of near bed concentration	(–)
D	=	Pipe diameter	(m)
d	=	Diameter solids	(m)
d_{50}	=	Median diameter solids	(m)
E	=	Erosion rate per unit width	(m/s)
f	=	Darcy–Weisbach flow resistance coefficient	(–)
g	=	Gravity	(m/s^2)
h_{bed}	=	Height bed layer observed visually	(m)
L	=	Length sawtooth wave	(m)
t	=	Time	(s)
U	=	Mean flow velocity	(m/s)
U_{cr}	=	Critical flow velocity for density wave development	(m/s)
u_*	=	Wall shear velocity	(m/s)
w	=	Fall velocity solitary particle	(m/s)
w_s	=	Fall velocity particles	(m/s)
w_{s0}	=	Average fall velocity of particles at bed level	(m/s)
x	=	Axial coordinate	(m)
z	=	Vertical coordinate	(m)
α	=	Variable slip coefficient	(–)
β	=	Hindered settling exponent	(–)
Δc	=	Maximum concentration difference sawtooth wave	(–)
ε	=	Axial dispersion	(m^2/s)
ρ	=	Density of mixture	(kg/m^3)
ρ_f	=	Density of fluid	(kg/m^3)
ρ_s	=	Density of solids	(kg/m^3)
ϕ	=	Dimensionless parameter	(m)
τ_w	=	Wall shear stress	(Pa)

References

1. ERCOLANI, D., FERRINI, F. and ARRIGONI, V. (1979). "Electric and Thermic Probes for Measuring the Limit Deposit Velocity." *Hydrotransport 6, Paper A3*, pp. 27–42.
2. KLOSE, R. (1984). "Influence of Particle Size Distribution on Pipeline Transport of Suspensions" ("Untersuchungen Zum Einfluss der Partikelgrossenverteilung auf den Rohrleitungstransport von Suspensionen" in German), Doctoral thesis, Technical University of Clausthal, Germany, pp. 130.
3. MATOUSEK, V. (1997). "Flow Mechanism of Sand–Water Mixtures in Pipelines." Doctoral Thesis, Delft University of Technology.
4. MATOUSEK, V. (2001). "On the Amplification of Density Waves in Long Distance Pipelines Connected with a Dredge." *Proceedings of the 16th World Dredging Congress (WODCON XVI "Dredging for Prosperity: Achieving*

Social and Economic Benefits)", Kuala Lumpur, Eastern Dredging Organisation.

5. MURAKAMI, Y., HIROSE, T. and ONO, S. (1985). "Mixing Loop Reactors, Encyclopedia of Fluid Mechanics." In: CHEREMISINOFF, N.P. (ed.), Dynamics of Single Fluid Flows and Mixing, Vol. 2. Chapter 22, Houston, Gulf Publishing, pp. 557–571.
6. NIEUWSTADT, F.T.M. and STEKETEE, J.A. (eds) (1995). *Selected Papers of J.M. Burgers*, Kluwer.
7. RHEE, C. van and TALMON, A.M. (2000). "Entrainment of Sediment (or Reduction of Sedimentation) at High Concentration." *10th International Conference on Transport and Sedimentation of Solid Particles*, Wroclaw, Poland.
8. TALMON, A.M. (1999). Mathematical Analysis of the amplification of Density Variations in Long-Distance Sand Transport Pipelines." *Proceedings of the Hydrotransport 14*, BHRG, Cranfield, UK, pp. 3–20.
9. TAYLOR, G.I. (1954). "The Dispersion of Matter in Turbulent Flow through a Pipe." *Proceedings of the Royal Society London, Series A, Mathematical and Physical Sciences*. London, pp. 446–468.
10. WINTERWERP, J.C. GROOT, M.B., de, MASTBERGEN, D.R. and VERWOERT, H. (1990). "Hyperconcentrated Sand–Water Mixture Flows Over Flat Bed." *J. Hydraulic Engrg. ASCE* 116(1), 36–54.